Detailed experimental study on intermediate-energy Coulomb excitation of ^{46}Ar

A. Gade,[1,2] D. Bazin,[1] C. M. Campbell,[1,2] J. A. Church,[1,2] D. C. Dinca,[1,2] J. Enders,[1,*] T. Glasmacher,[1,2] Z. Hu,[1,†] K. W. Kemper,[3] W. F. Mueller,[1] H. Olliver,[1,2] B. C. Perry,[1,2] L. A. Riley,[4] B. T. Roeder,[3] B. M. Sherrill,[1,2] and J. R. Terry[1,2]

[1] *National Superconducting Cyclotron Laboratory, Michigan State University, East Lansing, Michigan 48824, USA*

[2] *Department of Physics and Astronomy, Michigan State University, East Lansing, Michigan 48824, USA*

[3] *Department of Physics, Florida State University, Tallahassee, Florida 32306, USA*

[4] *Department of Physics and Astronomy, Ursinus College, Collegeville, Pennsylvania 19426, USA*

(Received 18 April 2003; published 21 July 2003)

Intermediate-energy Coulomb excitation is a key method to investigate collectivity in exotic nuclei far from β stability. We report on the measurement of the absolute $B(E2;0_1^+\rightarrow 2_1^+)$ excitation strength in ^{46}Ar for five different minimum impact parameters. Our findings underline the validity, feasibility, and perspective of this technique for the study of exotic nuclei also in the regime of higher beam energy.

DOI: 10.1103/PhysRevC.68.014302 PACS number(s): 25.70.De, 27.40.+z

I. INTRODUCTION

Coulomb excitation is a well established and widely used experimental technique to explore nuclear structure especially under the aspect of quadrupole collectivity in even-even nuclei [1–3]. In the dawn of this method stable target nuclei were excited in the Coulomb field of impinging stable heavy-ion beams at ''safe'' sub-barrier energies. In the last decade properties of nuclei beyond the valley of β stability merged into the focus of nuclear structure research. The availability of high-energy exotic beams prompted the development of intermediate-energy Coulomb excitation as a probe to investigate hardly accessible nuclear species very far from stability [4,5]. In inverse kinematics exotic nuclei are scattered off stable high-Z targets and are detected in coincidence with the deexcitation γ rays tagging the inelastic process (see, for example, Refs. [5–7]).

While beam energies *below* the Coulomb barrier prevent nuclear contributions to the excitation process, peripheral collisions have to be selected in the regime of intermediate-energy Coulomb excitation to ensure the dominance of the electromagnetic interaction. This can be accomplished by restricting the analysis to events at extremely forward scattering angles, corresponding to large impact parameters. For the first time we present a detailed experimental study of the interplay between impact parameters, angle-integrated cross sections and resulting $B(E2;0_1^+\rightarrow 2_1^+)$ excitation strengths in the framework of intermediate-energy Coulomb excitation of ^{46}Ar.

The $B(E2\uparrow)$ value of the short-lived ($T_{1/2}=7.8$ s) nucleus ^{46}Ar was first studied via intermediate-energy Coulomb excitation ^{46}Ar$+^{197}$Au at an average mid-target beam energy of 35 MeV/nucleon provided by the K1200 cyclotron at the National Superconducting Cyclotron Laboratory (NSCL) at the Michigan State University in 1996 [8]. A position-sensitive NaI(Tl) detector array [4,9] was used for the detection of the γ rays while the scattered particles were measured using a phoswich plastic scintillator with fixed opening angle. The present experiment was performed at the NSCL's new Coupled Cyclotron Facility (CCF) at higher beam energy (73 MeV/nucleon midtarget) using an array of highly segmented germanium detectors in combination with a high-resolution magnetic spectrograph.

II. EXPERIMENT

The 76.4 MeV/nucleon secondary beam ^{46}Ar was obtained by fragmentation of 110 MeV/nucleon ^{48}Ca primary beam impinging on a 376 mg/cm^2 ^{9}Be fragmentation target located at the midacceptance target position of the A1900 fragment separator [10]. The total momentum acceptance was reduced to 0.5% to provide a good separation of the ^{46}Ar fragments resulting in a purity of about 99%.

The secondary 209(4) mg/cm^2 ^{197}Au target was placed at the target position of the S800 spectrograph [11] and surrounded by SeGA (segmented germanium array), the largest operational highly-segmented germanium detector array for in-beam γ-ray spectroscopy with fast exotic beams. Fifteen 32-fold segmented HPGe detectors [12] were arranged at a distance of 20 cm from the target in two rings with central angles of 90° and 37° relative to the beam axis. The high degree of segmentation allowed for an accurate event-by-event Doppler reconstruction of the γ rays emitted in flight. The configuration with eight detectors in the 90° ring and seven in the 37° ring provided a total photo-peak efficiency of 2.0% at 1.33 MeV γ-ray energy. GEANT3 [13] simulations successfully modeled the efficiency determined with the sources at rest and provided the detector response for in-beam data by taking into account the Doppler shifts arising from the velocity of the recoils at the moment of the γ-ray emission. The detector efficiency was also folded with the γ-ray angular distribution [3,19] in the projectile frame to determine the photopeak efficiency for a photon emitted from the Coulomb-excited projectile. In total, an uncertainty of 5% is assumed for the γ-ray efficiency. Figure 1 shows the γ spectrum detected with SeGA in coincidence with ^{46}Ar fragments. The energy of the 2_1^+ $E(2_1^+)=1555(9)$ keV state

*Present address: Institut für Kernphysik, TU Darmstadt, D-64289 Darmstadt, Germany.

†Present address: School of Medicine, University of Utah, Salt Lake City, UT 84112.

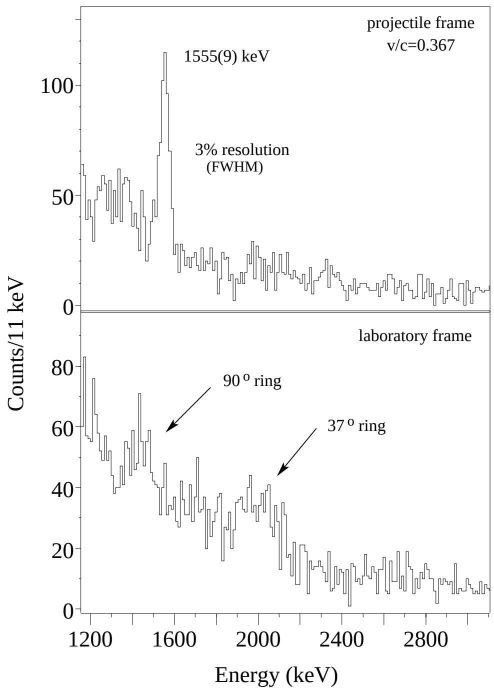

FIG. 1. Background-subtracted γ-ray spectra observed in the laboratory system (lower panel) and event by event Doppler reconstructed in the projectile frame (upper panel). The two Doppler-broadened bumps in the laboratory system correspond to the detection of the $2_1^+ \rightarrow 0_1^+$ 1555 keV transition of ^{46}Ar in the 90° ring and the 37° ring of SeGA, respectively.

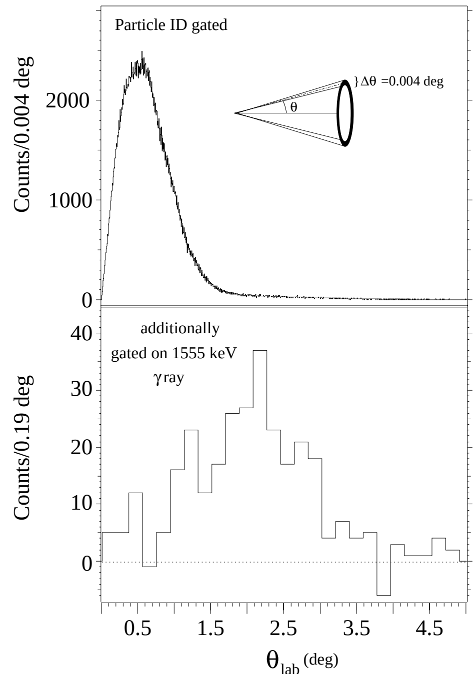

FIG. 2. Number of particles scattered into the annular solid angle segment $\Delta\Omega(\theta) = 2\pi \sin\theta\Delta\theta$ with bin width $\Delta\theta = 0.004°$ (upper panel) and 0.19° (lower panel). The scattering angle of ^{46}Ar is event-by-event reconstructed in the S800 spectrograph. In the lower panel, an additional gate is applied on the $2_1^+ \rightarrow 0_1^+$ γ-ray transition of ^{46}Ar (background subtracted).

is, by significantly reduced uncertainty, in good agreement with the value determined in the previous Coulomb-excitation measurement $E(2_1^+) = 1554(26)$ keV [8], and also agrees with $E(2_1^+) = 1550$ keV observed following the fragmentation of ^{48}Ca [14]. However, there is a discrepancy with $E(2_1^+) = 1577(1)$ keV quoted for ^{46}Ar in a heavy-ion multinucleon transfer experiment [15].

The particle identification and the determination of the scattering angle off the Au target were performed with the focal plane detector system of the high-resolution S800 spectrograph [11,16]. The energy loss in the S800 ion chamber and time-of-flight information taken between a beam-monitoring scintillator located in the A1900 extended focal plane and the scintillators in the spectrograph's focal plane were employed to unambiguously identify the reaction residues behind the gold target. The spectrograph was operated in focus mode, where the ^{46}Ar radioactive beam was momentum focused onto the reaction target. The two position-sensitive cathode readout drift counters of the S800 focal-plane detector system in conjunction with the optics code COSY [17] served to reconstruct the scattering angle on an event-by-event basis. In Fig. 2 the scattering angle spectra in the laboratory system are displayed. Given is the number of particles scattered into the annual solid angle segment $\Delta\Omega(\theta) = 2\pi \sin\theta\Delta\theta$, where $\Delta\theta$ is the width of the angle bin (see Fig. 2 inset, upper panel).

Applying gates $\{0°, \theta^{\max}\}$ on the scattering angle spectrum enabled the determination of angle-integrated cross sections σ for different maximum scattering angles $\theta^{\max}$. We used five different $\theta_{\rm lab}^{\max}$: 1.9°, 2.2°, 2.5°, 2.7°, and 2.9°. Our choice of $\theta^{\max}$ led to integrated cross sections between 32 and 68 mb (see the upper panel of Fig. 3). The accuracy of the reconstructed scattering angle is assumed to be 0.12° in the laboratory system limited by the angle resolution in

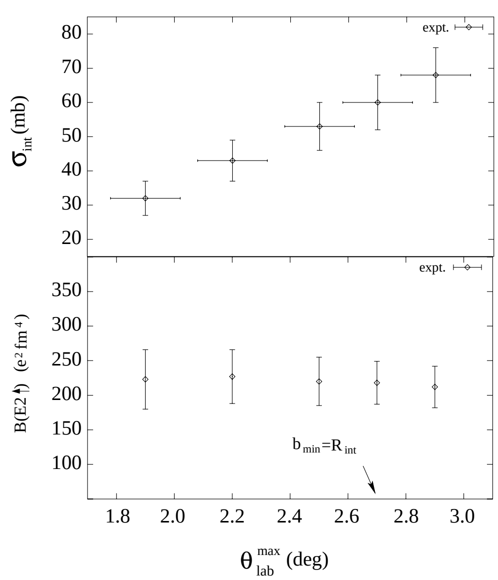

FIG. 3. Measured angle-integrated Coulomb excitation cross sections and deduced absolute $B(E2\uparrow)$ excitation strengths determined following the Winther/Alder theory of relativistic Coulomb excitation [19].

TABLE I. Experimental parameters and results.

$0° - \theta_{\rm lab}^{\rm max}$		$0°-1.9°$	$0°-2.2°$	$0°-2.5°$	$0°-2.7°$	$0°-2.9°$
$E(^{46}$Ar) midtarget (MeV/nucleon)	73.2					
^{46}Ar beam purity (%)	$\geqslant 99$					
Target ^{197}Au (mg/cm^2)	209					
Typical intensity on target (kHz)	13					
Total run time (h)	≈ 9					
Integrated cross section σ (mb)		32(5)	43(6)	53(7)	60(8)	68(8)
$b_{\rm min}$ (fm)		18.8	16.2	14.3	13.2	12.3
$R_{\rm int}$ (fm)	13.3					
$B(E2;0_1^+ \to 2_1^+)(e^2\ {\rm fm}^4)$		226(43)[a]	227(39)	220(35)	218(31)	212(30)
Adopted $B(E2\uparrow)(e^2\ {\rm fm}^4)$	218(31)					
$B(E2\uparrow)(e^2\ {\rm fm}^4)$ from Ref. [8]	196(39)					

[a]$B(E2)$ at $b_{\rm min} = R_{\rm int}$.

the focal plane of $\pm 0.06°$ [16] and systematic uncertainties attributed to the reconstruction procedure. The experimental parameters and results are summarized in Table I.

III. DISCUSSION

The Coulomb interaction is generally assumed to dominate in heavy-ion scattering processes whenever the minimum impact parameter $b_{\rm min}$ is larger than the electromagnetic interaction radius $R_{\rm int}$. For the present discussion we refer to the definition of $R_{\rm int}$ following Wilcke *et al.* [18]:

$$R_{\rm int} = C_t + C_p + 4.49 - \frac{C_p + C_t}{6.35} \quad ({\rm fm}), \tag{1}$$

$$C_i = R_i(1 - 1/R_i^2), \quad i = t,p, \tag{2}$$

$$R_i = 1.28 A_i^{1/3} - 0.76 + 0.8 A_i^{-1/3}, \tag{3}$$

with the nuclear radius R_i for a homogeneous (sharp) mass distribution, the nuclear radius C_i for a diffuse Fermi mass distribution, and the mass number A_i for the target t and projectile p, respectively. For the beam-target combination employed in the present experiment, $R_{\rm int}$ equals 13.3 fm. In the framework of relativistic Coulomb excitation the minimum impact parameter $b_{\rm min}$ and the maximum scattering angle in the center-of-mass system, $\theta_{\rm c.m.}^{\rm max}$ are related by [19,4]

$$b_{\rm min} = \frac{a}{\gamma} \cot(\theta_{\rm c.m.}^{\rm max}/2), \tag{4}$$

with

$$a = \frac{Z_{\rm proj} Z_{\rm tar} e^2}{m_0 c^2 \beta^2}, \tag{5}$$

$$\gamma = 1/\sqrt{1-\beta^2}, \quad \beta = v/c, \tag{6}$$

and m_0 the reduced mass of the projectile-target system.

The experimentally accessible observable to pinpoint the minimum impact parameter $b_{\rm min}$ is obviously the maximum scattering angle $\theta^{\rm max}$. Using the theory of relativistic Coulomb excitation [19], we determined absolute $B(E2\uparrow)$ values from the measured angle-integrated cross sections (see lower panel of Fig. 3). The uncertainty in the scattering angle translates into a systematic error of 10%, 9%, 8%, 7%, and 7% for the $B(E2\uparrow)$ values determined for $\theta_{\rm lab}^{\rm max}$: 1.9°, 2.2°, 2.5°, 2.7°, and 2.9°, respectively, and is included in the uncertainties quoted in Fig. 3 and Table I.

We found the $B(E2)$ strength to be constant over a broad range of impact parameters, 18.8 fm $\geqslant b_{\rm min} \geqslant$ 12.3 fm with $R_{\rm int}$ = 13.3 fm. Coupled channel calculations employing the code ECIS [20] (optical model potential from Ref. [21]) verified that the nuclear contribution to the cross sections is negligible in the angular range covered by the present experiment.

IV. SUMMARY

The absolute $B(E2;0_1^+ \to 2_1^+)$ excitation strength in ^{46}Ar has been measured in intermediate-energy Coulomb excitation at 73 MeV/nucleon mid-target beam energy for five different maximum scattering angles corresponding to five different minimum impact parameters.

For all selected maximum scattering angles, we extracted $B(E2)$ values which are consistent with each other and in agreement with a previous result obtained at a lower beam energy [8]. This proves the robustness of the analysis of intermediate-energy Coulomb excitation, making it a key-method for the investigation of exotic isotopes. Coulomb excitation will be particularly interesting for experiments at the rare-isotope facilities planned in Europe, Japan, and the U.S. in their quest to further reach out towards the drip lines.

ACKNOWLEDGMENTS

We thank A. Stolz, T. Ginter, M. Steiner, and the NSCL cyclotron operations group for providing the high-quality secondary and primary beams. This work was supported by the National Science Foundation under Grant Nos. PHY-0110253, PHY-9875122, and PHY-0098774.

[1] E.Z. Fermi, Z. Phys. **29**, 315 (1924).
[2] C.F. Weizsäcker, Z. Phys. **88**, 612 (1934).
[3] K. Alder, T. Huus, B. Mottelson, and A. Winther, Rev. Mod. Phys. **28**, 432 (1956).
[4] T. Glasmacher, Annu. Rev. Nucl. Part. Sci. **48**, 1 (1998).
[5] T. Motobayashi, Y. Ikeda, Y. Ando, K. Ieki, M. Inoue, N. Iwasa, T. Kikuchi, M. Kurokawa, S. Moriya, S. Ogawa, H. Murakami, S. Shimoura, Y. Yanagisawa, T. Nakamura, Y. Watanabe, M. Ishihara, T. Teranishi, H. Okuno, and R.F. Casten, Phys. Lett. B **346**, 9 (1995).
[6] T. Glasmacher, B.A. Brown, M.J. Chromik, P.D. Cottle, M. Fauerbach, R.W. Ibbotson, K.W. Kemper, D.J. Morrissey, H. Scheit, D.W. Sklenicka, and M. Steiner, Phys. Lett. B **395**, 163 (1997).
[7] O. Sorlin *et al.*, Phys. Rev. Lett. **88**, 092501 (2002).
[8] H. Scheit, T. Glasmacher, B.A. Brown, J.A. Brown, P.D. Cottle, P.G. Hansen, R. Harkewicz, M. Hellström, R.W. Ibbotson, J.K. Jewell, K.W. Kemper, D.J. Morrissey, M. Steiner, P. Thirolf, and M. Thoennessen, Phys. Rev. Lett. **77**, 3967 (1996).
[9] H. Scheit, T. Glasmacher, R.W. Ibbotson, and P.G. Thirolf, Nucl. Instrum. Methods Phys. Res. A **422**, 124 (1999)
[10] D. J. Morrissey, B. M. Sherrill, M. Steiner, A. Stolz, and I. Wiedenhöver, Nucl. Instrum. Methods Phys. Res. B **204**, 90 (2003).
[11] D. Bazin, J. A. Caggiano, B. M. Sherrill, J. Yurkon, and A. Zeller, Nucl. Instrum. Methods Phys. Res. B **204**, 629 (2003).
[12] W.F. Mueller, J.A. Church, T. Glasmacher, D. Gutknecht, G. Hackman, P.G. Hansen, Z. Hu, K.L. Miller, and P. Quirin, Nucl. Instrum. Methods Phys. Res. A **466**, 492 (2001).
[13] GEANT, version 3.21, CERN program library, long writeup W5013, 1994.
[14] F. Azaiez, Nucl. Phys. **A704**, 37c (2002).
[15] B. Fornal, R. Broda, W. Królas, T. Pawlat, J. Wrzesiński, D. Bazzacco, S. Lunardi, C. Rossi Alvarez, G. Viesti, G. de Angelis, M. Cinausero, D. Napoli, J. Gerl, E. Caurrier, and F. Nowacki, Eur. Phys. J. A **7**, 147 (2000).
[16] J. Yurkon, D. Bazin, W. Benenson, D.J. Morrissey, B.M. Sherrill, D. Swan, and R. Swanson, Nucl. Instrum. Methods Phys. Res. A **422**, 291 (1999).
[17] M. Berz, K. Joh, J.A. Nolen, B.M. Sherrill, and A.F. Zeller, Phys. Rev. C **47**, 537 (1993).
[18] W.W. Wilcke, J.R. Birkelund, H.J. Wollersheim, A.D. Hoover, J.R. Huizenga, W.U. Schröder, and L.E. Tubbs, At. Data Nucl. Data Tables **25**, 391 (1980).
[19] A. Winther and K. Alder, Nucl. Phys. **A319**, 518 (1979).
[20] J. Raynal, Phys. Rev. C **23**, 2571 (1981).
[21] T. Suomijärvi, D. Beaumel, Y. Blumenfeld, Ph. Chomaz, N. Frascaria, J.P. Garron, J.C. Roynette, J.A. Scarpaci, J. Barrette, B. Fernandez, J. Gastebois, and W. Mittig, Nucl. Phys. **A509**, 369 (1990).